Growth of ultrathin pentacene films on polymeric substrates

Primož Rebernik Ribič,[1] Vivek Kalihari,[2] C. Daniel Frisbie,[2] and Gvido Bratina[1]
[1]*Laboratory for Organic Matter Physics, University of Nova Gorica, Vipavska 11c, 5270 Ajdovščina, Slovenia*
[2]*Department of Chemical Engineering and Materials Science, University of Minnesota, 151 Amundson Hall, 421 Washington Avenue SE, Minneapolis, Minnesota 55455, USA*
(Received 23 March 2009; revised manuscript received 6 July 2009; published 10 September 2009)

Growth of vapor deposited submonolayer thick pentacene films on polystyrene, poly(α-methylstyrene), and poly(methyl methacrylate) was investigated using tapping-mode atomic force microscopy. For comparison we also studied pentacene thin-film growth on SiO_2. On polar surfaces pentacene nucleates in the form of two-dimensional islands, while on apolar surfaces at higher temperatures a noticeable fraction of three-dimensional island nucleation is also observed. By measuring the monolayer-island nucleation densities and coverages as a function of substrate temperature, we showed that a transition from complete to the initially incomplete condensation occurs in the temperature range from 45 to 55 °C on all surfaces. We calculated the activation energies for surface diffusion of pentacene molecules on all substrates. From the temperature dependence of the first and subsequent pentacene layer coverages we deduced that the substrate-pentacene interaction is weaker in the case of apolar surfaces as compared to polar surfaces. Our findings suggest that it is possible to predict the submonolayer nucleation behavior of pentacene on inert substrates based on the polar component of the substrate surface energy.

DOI: 10.1103/PhysRevB.80.115307 PACS number(s): 81.15.Ef, 81.15.Aa, 68.43.Jk, 72.80.Le

I. INTRODUCTION

Mechanical flexibility and low temperature processability of organic semiconductor thin films are considered some of the main practical advantages of using organic semiconductors as active layers in electronic devices such as organic thin-film transistors (OTFTs). Pentacene, a member of the oligoacene family, stands out as one of the more attractive candidates for OTFT applications on account of its relatively high charge carrier mobility[1,2] and its ability to form ordered polycrystalline films on a variety of substrates.[3–7] In order to fully exploit the mechanical flexibility of organic materials in OTFTs, the active layer has to be deposited on a flexible surface such as a polymeric substrate. Consequently, an increasing number of OTFT studies involve vapor deposition of thin pentacene films on polymeric dielectrics.[8–12]

Studies of charge carrier transport have shown[13,14] that conduction in OTFTs involves one or at most two layers of the active organic material. It is therefore reasonable to expect that the performance of pentacene transistors will strongly depend on the morphology of the starting layers. The morphology of ultrathin (~1 nm) polycrystalline pentacene films is characterized by grains with densities that depend on the substrate temperature and deposition rate. In order to gain a better understanding of the mechanism of charge carrier transport in ultrathin pentacene films a thorough investigation of their morphology as a function of deposition parameters is necessary. Up to now, only a few (somewhat contradictory) morphological studies of ultrathin pentacene films on polymeric substrates have been reported.[7,9,15]

In the following work we present a detailed analysis of ultrathin pentacene film nucleation on three different polymeric dielectrics: polystyrene—PS, poly(α-methylstyrene)—PαMS, and poly(methyl methacrylate)—PMMA. These three materials were chosen because it was possible to obtain surfaces with the same root-mean-square (rms) roughness for all types of dielectrics. This is especially important because the substrate rms roughness may substantially influence the surface nucleation densities of pentacene grains.[15,16] Since these polymeric dielectrics are characterized either by a polar (PMMA) or an apolar (PS, PαMS) surface, it was possible to study the nucleation behavior of pentacene as a function of the polar character of the substrate surface. Different growth behavior at higher temperatures was observed on apolar surfaces as compared to polar surfaces. For comparison, the nucleation of pentacene on SiO_2, a commonly used dielectric in OTFT studies, was also investigated. The nucleation regime of pentacene on all of these substrates was unambiguously identified from plots of submonolayer nucleation densities and coverages as a function of deposition parameters. This allowed us to calculate the energy barriers for surface diffusion of pentacene molecules.

II. EXPERIMENTAL

Molecular weights (M_W) and nominal glass transition temperatures (T_g) of polymers (Aldrich, Polymer Source Inc.) used in this study are listed in Table I.

Thermally grown SiO_2 was used as a substrate for polymer thin-film preparation. The SiO_2 substrates were sonicated in isopropanol for 10 min and dried with nitrogen gas. Polymeric surfaces were prepared by spin coating the sub-

TABLE I. Molecular weights and nominal glass transition temperatures of PS, PαMS, and PMMA.

Polymer	PS	PαMS	PMMA
M_W [kg/mol]	350	838	996
T_g [°C]	95	≈180 From Ref. 33	125

TABLE II. Surface properties of substrates. The uncertainties in the surface energies are a result of the fitting procedure (see, e.g., Ref. 18).

Substrate	Water contact angle (deg)	Dispersive component of surface energy (mJ/m^2)	Polar component of surface energy (mJ/m^2)	Total surface energy (mJ/m^2)
PS	90 ± 2	38.4 ± 7.8	0.6 ± 1.3	39.0 ± 9.1
PαMS	91 ± 2	40.5 ± 5.7	0.4 ± 0.6	40.9 ± 6.3
PMMA	71 ± 2	28.9 ± 8.5	8.3 ± 4.7	37.3 ± 13.2
SiO_2	37 ± 2	26.6 ± 6.7	30.9 ± 7.5	57.5 ± 14.2

strates with 1 wt. % toluene solutions at 4000 rpm. The resulting polymer film thicknesses were approximately 40 nm in all cases. The substrates were then left to dry overnight at room temperature (RT) in an inert atmosphere. The rms surface roughness of the substrates was measured over a 4×4 μm^2 area with a Veeco CPII atomic force microscope (AFM), which was operated in tapping mode.

The surface energies of polymers were estimated by a technique proposed by Owens and Wendt.[17,18] The method is based on contact angle measurements of different characterization liquids on the substrate surface. The contact angle θ of a liquid drop on a solid surface is related to the energies of the liquid surface (γ_L), solid surface (γ_S), and the solid-liquid interface (γ_{SL}) according to the Young equation,[19]

$$\gamma_S = \gamma_{SL} + \gamma_L \cos\theta. \tag{1}$$

In general, the surface energy γ arises due to polar (dipole-dipole and dipole-induced dipole) and dispersive (induced dipole-induced dipole) interactions at the surface. Assuming that both the surface energy of a liquid and a solid can be written as a sum of their polar (γ^p) and dispersive (γ^d) components ($\gamma = \gamma^p + \gamma^d$), Owens and Wendt proposed the following semiempirical formula to calculate γ_{SL},[17]

$$\gamma_{SL} = \gamma_S + \gamma_L + 2(\sqrt{\gamma_L^d \gamma_S^d} + \sqrt{\gamma_L^p \gamma_S^p}). \tag{2}$$

By combining Eqs. (1) and (2) one obtains the following linear relation:

$$y = x\sqrt{\gamma_S^p} + \sqrt{\gamma_S^d},$$

where

$$y = -\frac{(1+\cos\theta)\gamma_L}{2\sqrt{\gamma_L^d}} \quad \text{and} \quad x = \sqrt{\frac{\gamma_L^p}{\gamma_L^d}}. \tag{3}$$

The values of x and y can be evaluated for a number of different liquids with known polar (γ_L^p) and dispersive (γ_L^d) components of the surface energy by measuring their contact angle on the substrate surface. The polar (γ_S^p) and dispersive (γ_S^d) components of the substrate surface energy are then obtained from the slope and intercept of the plot of $y(x)$. The total substrate surface energy is calculated as the sum of the polar and dispersive components. In our experiments, deionized water, diiodomethane, glycerol, and ethylene glycol were used as characterization liquids. The values of surface energies (γ_L), polar components (γ_L^p), and dispersive components (γ_L^d) for these liquids were taken from Refs. 17 and 18.

Submonolayer thick ($\approx$0.4 nm) pentacene (Fluka, 99.8%) films were grown by thermal evaporation in a vacuum chamber with a base pressure of $\leq 10^{-7}$ Torr. For the temperature dependence measurements of pentacene island densities and coverages, a temperature range from 10 to 60 °C was chosen. At temperatures near 70 °C high desorption rates resulted in no pentacene molecules being adsorbed onto the polymeric surfaces. The temperature of the substrates was controlled with a heating/cooling block attached to the sample holder. During each deposition all four types (PS, PαMS, PMMA, and SiO_2) of substrates were placed onto the sample holder simultaneously. Small samples (few mm^2) were used in order to avoid the angular dependence of the flux of pentacene molecules that strike the substrate surface. The morphology of submonolayer thick pentacene films was examined with a Veeco CPII AFM in tapping mode.

The pentacene island density at each temperature was obtained by summing the number of pentacene islands from a series of $\sim$10 AFM images, each containing $\sim$150 islands, and dividing the result by the total surface area. The pentacene coverage at each temperature was calculated from a series of $\sim$10 AFM images.

III. RESULTS AND DISCUSSION

All of the polymeric dielectrics used in our study exhibit a similar surface morphology with an rms roughness of 2.8 ± 0.1 Å as determined from a series of 4×4 μm^2 AFM images. In the case of SiO_2 substrates the rms roughness was 2.1 ± 0.1 Å.

Table II lists the surface energies and water contact angles for all four types of substrates. The differences in the total surface energies of polymeric substrates are very small. On the other hand, there are significant differences between the polar components of the surface energy. PMMA has a much larger polar component as compared to PS and PαMS. Among all substrates SiO_2 has the largest polar component and the highest surface energy. The differences in the polar components of the surface energy are probably a result of the surface chemical structure, i.e., the polar character of PMMA and SiO_2 substrates arises due to the exposure of oxygen containing groups at the surface. For further discussion it will be useful to group the surfaces according to their polar component of surface energy. We will refer to PMMA and SiO_2 as polar surfaces and PS and PαMS as apolar surfaces.

Figure 1 shows 4×4 μm^2 AFM topography images of submonolayer thick pentacene films deposited on all four

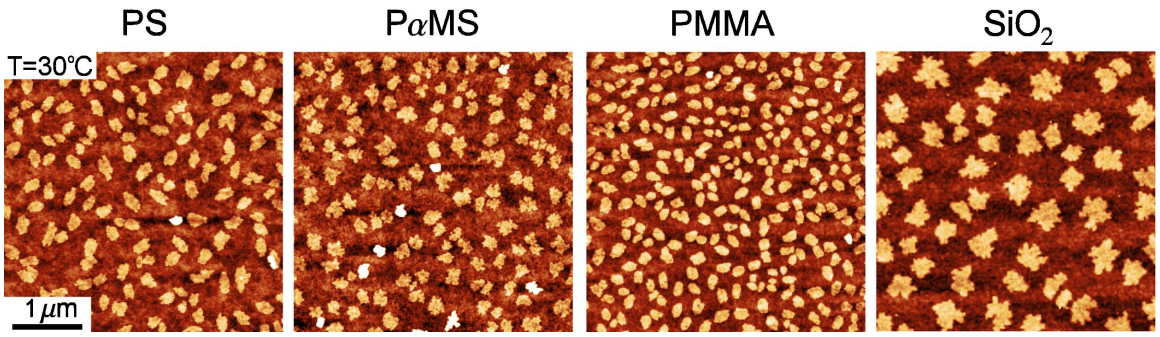

FIG. 1. (Color online) AFM height images of submonolayer thick (≈0.4 nm) pentacene films on PS, PαMS, PMMA, and SiO_2. The deposition rate was ≈0.4 nm/min in all cases.

types of substrates. The deposition rate and substrate temperature were fixed at ≈0.4 nm/min and 30 °C, respectively. Deposition was carried out simultaneously for all samples and was terminated when the quartz thickness monitor read ≈0.4 nm. Thus, the integrated flux (dose) of pentacene was the same for all substrates. In all cases the thin-film morphology is characterized by two-dimensional (2D) islands that measure ≈1.5 nm in height. The island height corresponds to standing pentacene molecules. This is consistent with previous observations of pentacene monolayer-island nucleation on inert substrates.[7,20–22] The shape of the islands is more compact in the case of PS and PMMA compared to PαMS and SiO_2. Later on we will argue that the compact island shapes on PS and PMMA are a consequence of a lower surface diffusivity of pentacene molecules on these two substrates as compared to the surface diffusivity of pentacene on PαMS. On the other hand, the fractal island shapes observed on SiO_2 may be a consequence of the lower surface roughness of SiO_2 compared to the polymer substrates. Clearly the nucleation density is lowest in the case of SiO_2, followed by PS and PαMS, with similar nucleation densities. The highest nucleation density of pentacene islands is observed on PMMA. On all polymeric substrates we note a small fraction of 3D pentacene islands (brighter islands in Fig. 1).

We investigated the temperature dependence of the coverage of first and subsequent pentacene layers as well as the temperature dependence of the pentacene island density in the range from 10 to 60 °C at a fixed deposition rate of ≈0.4 nm/min and fixed overall dose. Coverage of the first pentacene layer represents the pentacene island coverage, while coverage of subsequent layers is a measure of the degree of 3D island nucleation. The results are shown in Fig. 2.

Concentrating on the temperature dependence of the first pentacene layer coverage [Fig. 2(a)], we see that it is a slowly varying function of temperature in the range from 10 to ≈50 °C on all substrates. At RT (25 °C) maximum first monolayer coverage is observed for PMMA substrates (29.3%), followed by SiO_2 (26.9%), PS (23.4%), and PαMS (22.3%), respectively. The variation in coverage for equivalent integrated fluxes of pentacene indicates that the incoming molecules have different sticking coefficients on different substrates. In particular, the sticking coefficient of pentacene is higher on polar surfaces than on apolar surfaces. Turning back to Fig. 2(a), we see that the coverage exhibits a rapid decrease at temperatures above ≈50 °C. On all polymeric surfaces the coverage of the first pentacene layer decreases to zero at ≈70 °C [not shown in Fig. 2(a)].

If we now turn to the coverage of the second and subsequent pentacene layers [Fig. 2(b)], we observe that the polar character of the surface plays an important role. For the two polar (PMMA and SiO_2) surfaces the coverage of the second and subsequent pentacene layers is almost constant (below 1%) in the whole temperature range and only slightly increases at temperatures below 20 °C. For PMMA the coverage is highest at 15 °C (0.7%), while on SiO_2 maximum coverage is observed at 10 °C (0.3%). The fact that the coverage of the second and subsequent pentacene layers does not change significantly with temperature is a sign that 3D nucleation on PMMA and SiO_2 is an accidental occurrence in the temperature range from 10 °C to 60 °C; i.e., 3D islands have likely nucleated on defects.

The situation is different on apolar surfaces. The coverage of the second and subsequent pentacene layers exhibits a minimum at 25 °C on both PS (0.1%) and PαMS (0.4%). Above 25 °C, an increase (more pronounced on PαMS) in the coverage of the second and subsequent pentacene layers with temperature is observed. This is a clear indication that on apolar surfaces at higher temperatures (above ≈30 °C) a noticeable fraction of pentacene nucleates in 3D islands. At low temperatures (below 25 °C) the coverage of the second and subsequent pentacene layers slightly increases with decreasing temperature. The degree of 3D nucleation on apolar surfaces at low temperatures is comparable to that on polar surfaces. This again suggests nucleation on defects as the reason behind 3D island formation. At higher temperatures the degree of 3D island nucleation is significantly higher on apolar surfaces (especially on PαMS). We will show below that this is a consequence of a weaker substrate-pentacene interaction in the case of apolar surfaces.

As pointed out by Verlaak *et al.*,[23] the growth mode (2D or 3D) of organic semiconductors on inert substrates significantly depends on the deposition parameters (deposition rate and substrate temperature). The thermodynamic driving force of the nucleation process is the difference $\Delta\mu$ between the chemical potential of the vapor phase μ_v and the chemical potential of an infinitely large organic crystal μ_c ($\Delta\mu = \mu_v - \mu_c$). In calculating the energy released during molecular transfer from the vapor to the solid phase the finite size of the crystallites and the substrate-molecule interaction has to

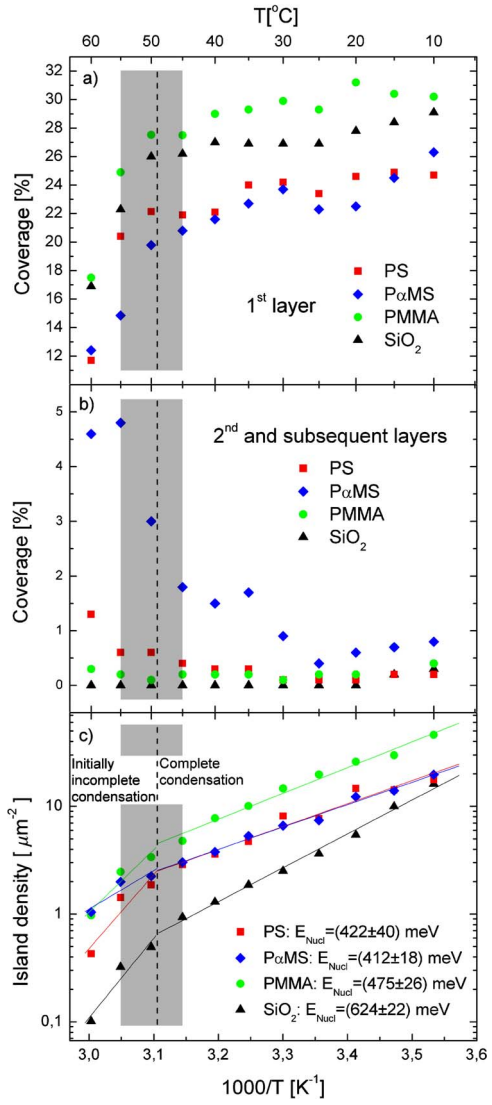

FIG. 2. (Color online) Coverage of (a) the first and (b) subsequent layers of pentacene as a function of substrate temperature for PS, PαMS, PMMA, and SiO_2. (c) Temperature dependence of the pentacene island density for all four types of substrates. Solid lines represent a fit of Eq. (4) to the experimental data. The activation energies E_{Nucl} in the complete condensation regime were calculated for all four substrates from the numerical fit in the temperature range from 10 to 45 °C. The vertical dashed line separates the two data sets that were used in the fitting procedure to extract the activation energies for homogeneous nucleation in the complete and initially incomplete condensation regimes (for the values of activation energies E_{Nucl} in the initially incomplete condensation regime see text). The shaded regions in all figures indicate the temperature window of transition between the two condensation regimes. For all of the above experiments, the total pentacene dose (integrated flux) was kept constant.

be taken into account. The parameter window for 3D nucleation strongly depends on the substrate-molecule interaction. At supersaturation ($\Delta\mu > 0$) and low substrate-molecule interactions, a transition from purely 2D to a combination of 3D and 2D growth is achieved by increasing the substrate temperature and/or by lowering the deposition rate. Further increase of the substrate temperature results in a purely 3D growth mode. The parameter window for 3D nucleation narrows with increasing substrate-molecule interaction. When the substrate-molecule interaction is larger or equal to the interaction of a single molecule with a neighboring molecular layer, only 2D growth is possible.

Taking these considerations into account we conclude that the substrate-pentacene interaction is weaker on apolar surfaces as compared to polar surfaces, since increasing the substrate temperature results in growth of 3D islands on the surface of PS and PαMS. In general there are two main contributions to the substrate-molecule interaction, the dispersion and the polar interactions. Referring to Table II, if both types of interactions contribute equally to the total interaction between the pentacene molecule and the substrate surface, one would expect a similar substrate-pentacene interaction for all the polymeric substrates. This is contrary to what we observe; however, we have not taken into account the high polarizability of pentacene molecules along the long molecular axis.[24] Since our results indicate a stronger substrate-pentacene interaction in the case of polar substrates, this suggests that the electrostatic interactions involving the pentacene induced dipole moment dominate during adsorption of pentacene on inert substrates. The incoming pentacene molecules mostly sense the polar groups exposed at the surface. High polarizability along the long molecular axis can also explain favorable interactions of the surface with standing pentacene molecules. The above observations are important because they show that the growth behavior of pentacene molecules on inert substrates depends on the polar component of the substrate surface energy and not just on the total surface energy (which is commonly believed). On surfaces with a bigger polar surface energy component, 2D growth mode can be maintained even at higher temperatures, whereas on surfaces with a smaller polar surface energy component, 3D growth may occur at elevated temperatures.

If we focus on the temperature dependence of the pentacene island density [Fig. 2(c)], we see that on all substrates the island density decreases rapidly with increasing substrate temperature. In order to explain this behavior we will turn to the mathematical model of nucleation and growth of thin films that has been developed by several authors (for a review of the theory see Ref. 25). The model is based on kinetic rate equations, which take into account different processes that may occur on the substrate surface, such as: surface diffusion, re-evaporation from the substrate surface, and island nucleation. Each of these processes is associated with an energy barrier (activation energy), e.g., formation of an island of a critical size i (islands with $i+1$ molecules are stable) involves a binding energy E_i, which is defined as the difference in free energy between i noninteracting molecules adsorbed on a surface and i molecules that form an island. Based on the relative time scales of various processes occurring on the substrate surface, the rate equation formalism can be used to predict different regimes of condensation. In the so called "complete condensation" regime, re-evaporation from the substrate surface is neglected. After steady state conditions are reached (the density of single molecules on the substrate surface is constant with respect to time), the incoming molecules that strike the substrate surface diffuse

on the substrate until they encounter a stable island. In the "initially incomplete" condensation regime, the islands also capture molecules by surface diffusion, although re-evaporation from the substrate surface cannot be neglected.

Based on the rate equation formalism, a general equation can be written for the dependence of the saturated island density N on the deposition rate R and substrate temperature T_S:

$$N \propto R^{\delta} \exp(E_{Nucl}/k_B T_S). \tag{4}$$

In the above equation k_B is the Boltzmann constant, E_{Nucl} is the activation energy for homogeneous nucleation, which includes activation energies for various surface processes, and δ is a critical exponent. The exact expressions for E_{Nucl} and the value of the critical exponent δ depend on the condensation regime, critical cluster size, and dimensionality of the clusters (2D or 3D), which all need to be determined in order to extract relevant parameters from the experimental data.

Both condensation regimes (initially incomplete and complete) were reported in previous studies of pentacene growth on inert surfaces. Based on the observations of pentacene monolayer-island nucleation on polymeric and inorganic substrates, Pratontep *et al.* concluded that the condensation regime of pentacene on PMMA and SiO_2 is initially incomplete.[7] On the other hand Stadlober *et al.*[15] argued that re-evaporation of molecules from the surface is not important, leading them to conclude that on polymeric surfaces and also on SiO_2 the condensation regime is complete. For temperature dependence measurements both Pratontep and Stadlober covered approximately the same temperature window (from 25 to 75 °C), but worked under slightly different deposition rates (0.4–0.5 nm/min vs 0.1 nm/min). In our experiments, we chose a temperature resolution of 5 °C. This allowed us to obtain more data points and observe any possible changes in the activation energies, which would suggest a change in the condensation regime. Indeed, unlike previous studies, our results indicate that in the temperature range from 10 to 60 °C at a deposition rate of ≈0.4 nm/min there is a transition from complete to the initially incomplete condensation regime.

In Fig. 2(c) we fitted Eq. (4) to the temperature dependence of the pentacene island density N. This allowed us to extract the nucleation energies E_{Nucl} for all four types of substrates. In the range 10 °C$\leq T_S <$ 50 °C the activation energies do not change with temperature, which is an indication of a single condensation regime in this temperature range. The activation energies for all substrates in this temperature range are listed in Fig. 2(c) (data points in the range 10 °C$\leq T_S \leq$45 °C were used in the numerical fit). We can identify the condensation regime by noting that in this temperature range the island coverage [Fig. 2(a)] does not change significantly with temperature. This is an indication that re-evaporation of pentacene molecules plays a minor role, which is characteristic of the complete condensation regime. In this regime the activation energy for nucleation E_{Nucl} has the following parameter dependencies in the case of 2D nucleation:[25]

TABLE III. Activation energies for diffusion of pentacene molecules on PS, PαMS, PMMA, and SiO_2.

Substrate	PS	PαMS	PMMA	SiO_2
E_D [meV]	403 ± 67	387 ± 30	492 ± 44	740 ± 37

$$E_{Nucl} = (E_i + iE_D)/(i+2), \tag{5}$$

where E_D is the activation energy for diffusion. In order to calculate E_D the critical cluster size i and the binding energy E_i must be known. Ruiz *et al.* have independently determined that the critical cluster size for pentacene on SiO_2 (complete condensation regime) is 3 by a scaling analysis of the island size distributions as a function of coverage.[26] A critical cluster size of 3 means that four pentacene molecules are necessary to form a stable island. A similar behavior in the case of complete condensation was observed by Stadlober *et al.* for pentacene on SiO_2 and polymeric substrates (PMMA, PVP, and PVCi).[15] They found that the critical cluster size is $3 \leq i \leq 4$.

In order to estimate the activation energies for diffusion we will assume, for the moment, that the critical cluster size is 3 for all substrate types. For $i=3$ the binding energy E_i is obtained by calculating the (free) energy difference between three noninteracting (freely-diffusing) pentacene molecules adsorbed on a surface and three molecules that form an island. Kalihari *et al.* have shown that the free energy of a three molecule cluster is ≈980 meV (see supplementary information in Ref. 27). The energy of three freely-diffusing pentacene molecules is approximated to be $3k_B T_D$, where T_D is the temperature at which pentacene molecules start desorbing from the substrate surface. The plot in Fig. 2(a) indicates that, on all types of surfaces, desorption of pentacene becomes important at temperatures above ≈50 °C. Using T_D=50 °C for the onset of desorption, the energy of three freely-diffusing pentacene molecules is estimated to be ≈80 meV. Kalihari *et al.* reported a value of 60 °C for T_D in the case of pentacene on SiO_2; however, the result was based on the analysis of fully coalesced pentacene monolayers, where interisland interaction may affect the desorption rate to a different extent than in the case of isolated monolayer islands. By taking the difference between the above two energies the binding energy $E_i \approx 900$ meV is obtained. Note that in this approximation the binding energy does not depend on the substrate type, because we observe the onset of desorption at similar temperatures on all surfaces. This is in agreement with the assumption of Pratontep *et al.*, who argued that E_i depends mainly on the structure of the critical island and not on the type of the substrate.[7] Using the above data, we calculated the activation energy for diffusion of pentacene molecules on PS, PαMS, PMMA, and SiO_2. The energies are listed in Table III.

We now turn back to the discussion of island shapes observed in Fig. 1. During growth of submonolayer thick films, the monolayer-island shapes are determined by the ratio of surface diffusivity/edge diffusivity (see, e.g., Ref. 28). It is reasonable to expect that the energy barrier for edge diffusion should be similar on all substrates as it mainly depends

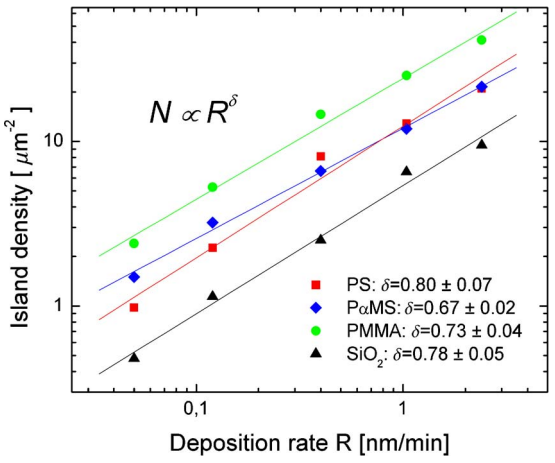

FIG. 3. (Color online) Pentacene island density as a function of deposition rate for PS, PαMS, PMMA, and SiO_2. The substrates were held at 30 °C.

on the intermolecular interactions. On the other hand, the activation energies for surface diffusion are different for different substrates (see Table III). If the activation energy for surface diffusion increases (i.e., the surface diffusivity decreases) the molecules at the island edges have more time to find energetically favorable positions around the island and this results in thermodynamically favorable compact islands. This observation is consistent with the activation energy data in Table III, with the exception of SiO_2. However, it should be noted that the surface diffusivity does not depend only on the activation energy for diffusion but also on the jump length.[29] In the case of diffusion of atoms on a crystalline surface the jump length is defined as the distance between nearest neighbor sites, while on amorphous substrates it can be assumed to be the mean free distance traveled before being scattered by a surface defect site. This would suggest that on surfaces with a lower rms roughness the jump length would be longer, which would imply the longest jump length on SiO_2 (lowest rms roughness). Since the diffusion constant varies as[29] $D \propto l^2$, where l is the jump length, this could result in a higher surface diffusivity of pentacene on SiO_2 as compared to other substrates, despite the fact that the activation energy for surface diffusion is highest on SiO_2. A high surface diffusivity of pentacene molecules on SiO_2 would explain the fractal island shapes observed in Fig. 1.

In the above calculation of activation energies for diffusion we assumed a critical cluster size of 3. We tried to confirm this assumption experimentally. In the complete condensation regime (2D case) the critical exponent $\delta = i/(i+2)$, which equals 0.6 in the case of $i=3$. We determined the critical exponents for pentacene on PS, PαMS, PMMA, and SiO_2 by measuring the deposition rate dependence of pentacene island density at a substrate temperature of 30 °C. The results are shown in Fig. 3. We calculated the critical exponents by fitting Eq. (4) to the experimental data. The critical exponents are in the range from 0.67 to 0.80 which is in reasonable agreement with the theoretical prediction of 0.6 for $i=3$.

In Fig. 2(c) we observe a change in the activation energies E_{Nucl} on all substrates in the temperature range 45 °C $< T_S <$ 55 °C. This implies also a change in the condensation regime. From Fig. 2(a) it is evident that the pentacene island coverage rapidly decreases when the temperature is raised above ≈50 °C, which is an indication of pentacene re-evaporation from the substrate surface. This implies that the condensation regime changes from complete condensation at lower temperatures, to the initially incomplete condensation at higher temperatures, where re-evaporation of pentacene plays an important role. From Fig. 2(c) we can obtain only a crude estimate of the activation energies E_{Nucl} in the range from 50 to 60 °C because the data consist of only three points (at temperatures around 70 °C the island coverage decreases to ~0). The activation energies are ~1360, ~710, ~1150, and ~1470 meV for PS, PαMS, PMMA, and SiO_2, respectively. In the initially incomplete condensation regime the activation energy for nucleation E_{Nucl} has the following parameter dependencies in the case of 2D nucleation:[25]

$$E_{Nucl} = (E_i + iE_A)/2, \tag{6}$$

where E_A is the activation energy for desorption. For initially incomplete condensation Pratontep *et al.* reported a value of $i=2$ in the case of pentacene on SiO_2 and polymeric substrates.[7] The corresponding value of E_i was in the range from 600 to 700 meV. The above data can be used to estimate E_A using Eq. (6). If we assume an average value of 650 meV for E_i, the activation energies for desorption E_A are ~1035, ~385, ~825, and ~1145 meV for PS, PαMS, PMMA, and SiO_2, respectively. We must keep in mind that these are only rough estimates because a small number of data points was used in the numerical fit. Nevertheless, the smallest E_A for PαMS implies a weaker substrate-pentacene interaction as compared to pentacene on other substrates. This is clearly consistent with the observation of a noticeable fraction of 3D pentacene islands that nucleate on PαMS at higher temperatures. Due to a relatively larger substrate-pentacene interaction in the case of PS, PMMA, and SiO_2 the fraction of 3D islands on these surfaces is considerably smaller or even negligible (SiO_2).

Although a transition between the complete and initially incomplete condensation regimes for pentacene on inert substrates was not reported up to now, a change in the critical nucleus size was observed by Wu *et al.*,[30] who studied pentacene growth on silicon dioxide by supersonic molecular beam deposition. They observed that the critical nucleus size i changed from 3 to 2 above a threshold energy (5–6 eV) of the incoming molecules.

Plots in Fig. 2 provide some information on the mean diffusion distance X_S of pentacene molecules on the substrate surface before desorption. In the complete condensation regime (below ≈50 °C) re-evaporation from the substrate surface is negligible. This suggests that diffusing pentacene molecules attach to stable islands before being desorbed, which implies that X_S is larger than the typical distance d between pentacene islands. As the temperature increases d also increases (the pentacene island density decreases). Above ≈50 °C the condensation regime changes to the initially incomplete condensation. In this regime the diffusing molecules may desorb before reaching a stable island. This

suggests that with increasing temperature X_S eventually becomes comparable to or smaller than the typical distance between pentacene islands.

In Fig. 2 we notice that the transition between the two condensation regimes occurs at similar temperatures on all types of substrates. This is somewhat surprising because the transition temperature should depend on the substrate-pentacene interaction. Particularly, one would expect to observe a difference between the transition temperatures on polymeric substrates and SiO_2. The experimental data suggest that in the temperature window of transition ($45\ ^\circ C < T_S < 55\ ^\circ C$) the ratio of X_S/d is close to unity on all types of surfaces. The mean diffusion distance of pentacene molecules on the substrate varies as $X_s \propto \exp[(E_A - E_D)/2k_BT_S]$.[7] The typical distance between the islands may be obtained through $d \sim \sqrt{1/N} \propto \exp(-E_{Nucl}/2k_BT_S)$. This means that, in the complete condensation regime, the ratio of X_s/d varies as $X_s/d \propto \exp[(E_A/2 - E_D/5)/k_BT_S]$. We see that the ratio X_s/d does not solely depend on E_A, but on the difference $\Delta E = E_A/2 - E_D/5$. These energy differences are ~437, ~115, ~314, and ~424 meV for PS, PαMS, PMMA, and SiO_2, respectively. We see that, except in the case of PαMS, the value of ΔE only slowly varies with the substrate type, being almost identical for PS and SiO_2. Therefore it is not unusual for transition between the two condensation regimes to occur in a relatively small temperature window ($\approx 10\ ^\circ C$) on all substrates. The reason for a relatively large difference between ΔE for PαMS and other three types of substrates may lie in the fact that the growth mode of pentacene on PαMS at higher temperatures is not purely 2D, since a substantial fraction of 3D island nucleation is observed at $T_S > 45\ ^\circ C$. In the case of a mixed 2D/3D nucleation we cannot derive a simple expression for the dependence of X_S/d on the various activation energies.

Controlling the pentacene island density on the substrate surface is important from the technological point of view because grain boundaries may influence charge carrier transport through organic films.[31] We have seen that the pentacene island density can be controlled by varying the substrate temperature and deposition rate. In the case of polymeric substrates the pentacene island density is higher on polar PMMA as compared to apolar PS and PαMS. This is probably a result of a higher activation energy for diffusion of pentacene molecules on PMMA compared to PS and PαMS. The substrate surface roughness may also play an important role in determining the nucleation density. The lowest surface roughness of SiO_2 substrates may be the reason for the lowest pentacene nucleation density among all types of surfaces.

At this point it is necessary to compare our findings with the results of Yang *et al.*[32] who studied the effect of gate-dielectric surface energy on the morphology of pentacene films. They found that the grain size in pentacene films decreases (the grain density increases) with decreasing total surface energy (and decreasing polar component of surface energy) of the polymer gate dielectric. This is somewhat contradictory to our results; however, the authors of the study in Ref. 32 concentrated on thicker pentacene films (with thicknesses above one monolayer), where 3D nucleation is the dominant growth mode. In general, the nucleation of higher monolayers on top of the first pentacene monolayer differs from nucleation of the first pentacene monolayer on a dielectric surface (e.g., in Ref. 20 the authors report that the size of islands that nucleate on top of the first pentacene monolayer is substantially larger than the size of pentacene islands that have nucleated on the substrate surface).

IV. CONCLUSIONS

We carried out a detailed analysis of ultrathin pentacene film growth on polymeric surfaces. For comparison pentacene thin-film nucleation was also studied on SiO_2. By measuring the monolayer-island nucleation densities and island coverages as a function of substrate temperature, we showed that a transition from complete to the initially incomplete condensation regime occurs in a temperature window from 45 to 55 °C on all surfaces. We were able to extract the activation energies for surface diffusion of pentacene molecules on all substrates. Analysis of the first and subsequent pentacene layer coverages as a function of temperature showed that on apolar surfaces at substrate temperatures above $\approx 30\ ^\circ C$ a noticeable fraction of pentacene nucleates in the form of 3D islands. Such behavior was ascribed to a weaker substrate-pentacene interaction in the case of apolar surfaces as compared to polar surfaces. Our results suggest that it is possible to predict the growth behavior of pentacene on nonreactive surfaces based on the polar component of the substrate surface energy.

ACKNOWLEDGMENTS

We acknowledge helpful discussions with E. Pavlica, A. Petrović, and P. Škraba.

[1] H. Klauk, M. Halik, U. Zschieschang, G. Schmid, W. Radlik, and W. Weber, J. Appl. Phys. **92**, 5259 (2002).
[2] D. Knipp, R. A. Street, A. Völkel, and J. Ho, J. Appl. Phys. **93**, 347 (2003).
[3] J. H. Kang and X.-Y. Zhu, Appl. Phys. Lett. **82**, 3248 (2003).
[4] L. Floreano, A. Cossaro, D. Cvetko, G. Bavdek, and A. Morgante, J. Phys. Chem. B **110**, 4908 (2006).
[5] W. J. Huang, B. Q. Li, and J. M. Zuo, Surf. Sci. **595**, 157 (2005).
[6] H. Yanagisawa, T. Tamaki, M. Nakamura, and K. Kudo, Thin Solid Films **464-465**, 398 (2004).
[7] S. Pratontep, F. Nüesch, L. Zuppiroli, and M. Brinkmann, Phys. Rev. B **72**, 085211 (2005).
[8] K. N. Narayanan Unni, S. Dabos-Seignon, A. K. Pandey, and J.-M. Nunzi, Solid-State Electron. **52**, 179 (2008).
[9] C. Kim, A. Facchetti, and T. J. Marks, Science **318**, 76 (2007).
[10] T.-S. Huang, Y.-K. Su, and P.-C. Wang, Appl. Phys. Lett. **91**,

092116 (2007).
[11] S. Lee, B. Koo, J. Shin, E. Lee, H. Park, and H. Kim, Appl. Phys. Lett. **88**, 162109 (2006).
[12] M. Halik, H. Klauk, U. Zschieschang, T. Kriem, G. Schmid, W. Radlik, and K. Wussow, Appl. Phys. Lett. **81**, 289 (2002).
[13] M. Daraktchiev, A. von Mühlenen, F. Nüesch, M. Schaer, M. Brinkmann, M.-N. Bussac, and L. Zuppiroli, New J. Phys. **7**, 133 (2005).
[14] F. Dinelli, M. Murgia, P. Levy, M. Cavallini, F. Biscarini, and D. M. de Leeuw, Phys. Rev. Lett. **92**, 116802 (2004).
[15] B. Stadlober, U. Haas, H. Maresch, and A. Haase, Phys. Rev. B **74**, 165302 (2006).
[16] S. E. Fritz, T. W. Kelley, and C. D. Frisbie, J. Phys. Chem. B **109**, 10574 (2005).
[17] D. K. Owens and R. C. Wendt, J. Appl. Polym. Sci. **13**, 1741 (1969).
[18] A. Pietak, S. Korte, E. Tan, A. Downard, and M. P. Staiger, Appl. Surf. Sci. **253**, 3627 (2007).
[19] J. Israelachvili, *Intermolecular and Surface Forces*, 2nd ed. (Academic Press, London, 1992).
[20] P. R. Ribič and G. Bratina, J. Vac. Sci. Technol. B **25**, 1152 (2007).
[21] P. R. Ribič and G. Bratina, Surf. Sci. **602**, 1368 (2008).
[22] S. Pratontep, M. Brinkmann, F. Nüesch, and L. Zuppiroli, Phys. Rev. B **69**, 165201 (2004).
[23] S. Verlaak, S. Steudel, P. Heremans, D. Janssen, and M. S. Deleuze, Phys. Rev. B **68**, 195409 (2003).
[24] E. V. Tsiper and Z. G. Soos, Phys. Rev. B **68**, 085301 (2003).
[25] J. A. Venables, G. D. T. Spiller, and M. Hanbücken, Rep. Prog. Phys. **47**, 399 (1984).
[26] R. Ruiz, B. Nickel, N. Koch, L. C. Feldman, R. F. Haglund, A. Kahn, F. Family, and G. Scoles, Phys. Rev. Lett. **91**, 136102 (2003).
[27] V. Kalihari, E. B. Tadmor, G. Haugstad, and C. D. Frisbie, Adv. Mater. **20**, 4033 (2008).
[28] A. L. Barabási and H. E. Stanley, *Fractal Concepts in Surface Growth* (Cambridge University Press, Cambridge, England, 1995).
[29] G. Antczak and G. Ehrlich, Surf. Sci. Rep. **62**, 39 (2007).
[30] Y. Wu, T. Toccoli, N. Koch, E. Iacob, A. Pallaoro, P. Rudolf, and S. Iannotta, Phys. Rev. Lett. **98**, 076601 (2007).
[31] A. Di Carlo, F. Piacenza, A. Bolognesi, B. Stadlober, and H. Maresch, Appl. Phys. Lett. **86**, 263501 (2005).
[32] S. Y. Yang, K. Shin, and C. E. Park, Adv. Funct. Mater. **15**, 1806 (2005).
[33] M. G. D. van der Grinten, A. S. Clough, T. E. Shearmur, M. Geoghegan, and R. A. L. Jones, Polymer **39**, 3623 (1998).